CrossMark

Three gemini cationic surfactants as biodegradable corrosion inhibitors for carbon steel in HCl solution

Salah M. Tawfik[1] · **Ali A. Abd-Elaal**[1] · **Ismail Aiad**[1]

Abstract   Three gemini cationic surfactants with different hydrophobic spacer chain lengths were synthesized and characterized. The inhibition effect of N,N'-bis(2-hydroxyethyl)-N,N'-dimethyl-N,N'-bis(2-(tetradecanoyloxy)ethyl)ethane-1,2-diaminium bromide (G-2); N,N'-bis(2-hydroxyethyl)-N,N'-dimethyl-N,N'-bis(2-(tetradecanoyloxy)ethyl) hexane-1,6-diaminium bromide (G-6); and N,N'-bis(2-hydroxyethyl)-N,N'-dimethyl-N,N'-bis (2-(tetradecanoyloxy) ethyl) dodecane-1,12-diaminium bromide (G-12) on the corrosion of carbon steel in 1.0 M HCl solution at 25–60 °C was studied by weight loss, potentiodynamic polarization, and electrochemical impedance spectroscopy. The results show that the synthesized inhibitors are effective inhibitors even at very low concentration, and the adsorption on the carbon steel surface obeys the Langmuir adsorption isotherm. Potentiodynamic polarization curves reveal that the synthesized inhibitors behave as a mixed-type inhibitor. Adsorption of used inhibitors led to a reduction in the double layer capacitance and an increase in the charge transfer resistance. Thermodynamic parameters have been obtained by adsorption theory. Surface activity and corrosion inhibition relationship were discussed. The biodegradability of the synthesized surfactants showed their readily biodegradation in the open environment and were considered as environmentally friendly corrosion inhibitors.

Keywords   Gemini cationic surfactant · Carbon steel · Impedance · Mixed inhibitor · Thermodynamic · Surface activity · Biodegradable

✉   Salah M. Tawfik
     salahtwfk85@yahoo.com

[1]   Egyptian Petroleum Research Institute, Nasr City, Cairo, Egypt

⌖ Springer

Introduction

Carbon steel (CS) is used in large amounts in marine applications, chemical processing, petroleum production and refining, construction and metal processing equipment [1–4]. These applications usually induce serious corrosive effect on equipment, tubes, and pipelines made of iron and its alloys [5–7].

The use of inhibitors is one of the most convenient means for protection of steel corrosion in acidic solution as they can prevent metal from dissolution and consequently reduce the operation cost. The existing data showed that most organic compounds which were used as corrosion inhibitors can be adsorbed on metal surface via heteroatoms such as nitrogen, sulfur, oxygen, and phosphorus, multiple bonds or aromatic rings, and they block the active sites accordingly, thereby decreasing the corrosion rate [1, 8]. The inhibition efficiency of organic inhibitors is mainly dependent on its affinity and compatibility to the metal surface [9]. Various efficient organic inhibitors have heteroatoms and multiple bonds or aromatic rings in their structures. As a representative type of these organic inhibitors, quaternary ammonium salts have been demonstrated to be highly effective in corrosion inhibition for different aggressive media [10–12].

Surfactant corrosion inhibitors have many advantages such as high inhibition efficiency, low price, low toxicity, and easy production. In general, the inhibitory action of surfactant in aqueous solutions is due to a physical adsorption or chemisorption of surfactant molecules onto the metal surface, depending on the charge on the solid surface and the free energy change of transferring a hydrocarbon chain from water to the solid surface. The adsorption of a surfactant markedly changes the corrosion resisting property of a metal and for this reason, the study of the correlation between the adsorption and corrosion inhibition is of a considerable importance [13–19].

Gemini surfactants are a new generation of surfactants developed in recent years that consist of two hydrophilic and two hydrophobic groups and are separated by a spacer in a molecular structure. It has been demonstrated that this new surfactant exhibits properties superior to those of conventional surfactants, such as better solubility and greater effect in lowering the surface tension of water. During recent years, an increasing interest has been focused on the investigation of the inhibition behavior of gemini surfactants in various aggressive media [20, 21].

In the present paper, the efficiency of three novel gemini cationic surfactants namely: *N*,*N*′-bis(2-hydroxyethyl)-*N*,*N*′-dimethyl-*N*,*N*′-bis(2-(tetradecanoyloxy)ethyl) ethane-1,2-diaminium bromide (G-2); *N*,*N*′-bis(2-hydroxyethyl)-*N*,*N*′-dimethyl-*N*,*N*′-bis(2-(tetradecanoyloxy)ethyl) hexane-1,6-diaminium bromide (G-6); and *N*,*N*′-bis(2-hydroxyethyl)-*N*,*N*′-dimethyl-*N*,*N*′-bis(2-(tetradecanoyloxy)ethyl) dodecane-1,12-diaminium bromide (G-12) as corrosion inhibitors of CS in 1 M HCl was investigated by potentiodynamic polarization, electrochemical impedance spectroscopy, and weight loss methods. The thermodynamic parameters and activation energy of the inhibitor were studied.

Experimental and method

Materials

Tests were performed on CS of the following composition: 0.11 % C, 0.45 % Mn, 0.04 % P, 0.05 % S, 0.25 % Si, and the reminder is Fe.

Inhibitors

The used inhibitors were prepared through two steps:

Synthesis of N,N-bis(hydroxyethyl)-methylamine monoester

N,N-Bis(hydroxyethyl)-methylamine (0.1 mol) and tetradecanoic acid (0.1 mol) were esterified individually in the presence of xylene as a solvent and 0.01 % p-toluene sulphonic acid as a catalyst, until the azeotropic amount of water (0.1 mol, 1.8 mL) was removed. A vacuum rotary evaporator was used to remove the solvent. The excess residual materials were removed by means of vacuum distillation, Fig. 1 [22].

Synthesis of N,N′-bis(2-hydroxyethyl)-N,N′-dimethyl-N,N′-bis(2-(tetradecanoyloxy) ethyl)alkyl diaminium bromide

Synthesized gemini cationic surfactants were obtained by a coupling reaction between dibromoalkanes, namely: 1,2-dibromoethane, 1,6-dibromohexane, and 1,12-dibromododecane (0.1 mol) and the synthesized N,N-bis(hydroxyethyl)-methylamine monoester (0.1 mol) in 50 ml acetone. The reaction mixture was refluxed for 12 h and left for complete precipitation of the cationic compounds. The produced diquaternary ammonium salts were filtered off and recrystallized three times from acetone to produce the desired gemini cationic surfactants (**G-2, G-6 and G-12**) [23]. Figure 1 shows the synthetic route of the gemini cationic surfactants.

Solutions

The aggressive solution, 1.0 M HCl was prepared by dilution of analytical grade HCl (37 wt%) with distilled water. The concentration range of the synthesized inhibitors used varied from 5×10^{-5} to 5×10^{-3} M for corrosion measurements. Double distilled water was used for preparing test solutions in all measurements.

Potentiodynamic polarization measurement

Polarization experiments were carried out using a conventional three-electrode cell with a platinum counter electrode and a saturated calomel electrode (SCE) as a reference electrode. The working electrode was a rod of CS embedded in PVC
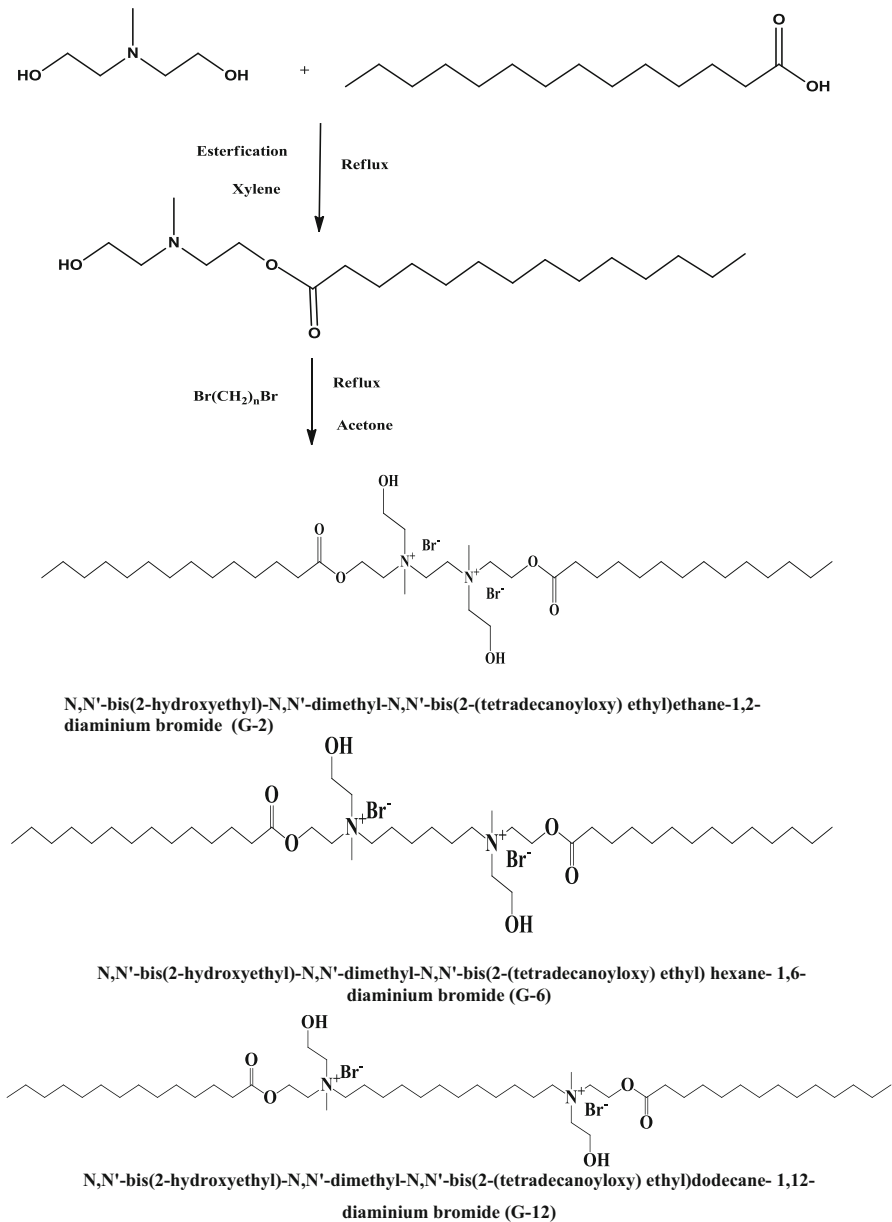
N,N'-bis(2-hydroxyethyl)-N,N'-dimethyl-N,N'-bis(2-(tetradecanoyloxy) ethyl)ethane-1,2-diaminium bromide (G-2)

N,N'-bis(2-hydroxyethyl)-N,N'-dimethyl-N,N'-bis(2-(tetradecanoyloxy) ethyl) hexane- 1,6-diaminium bromide (G-6)

N,N'-bis(2-hydroxyethyl)-N,N'-dimethyl-N,N'-bis(2-(tetradecanoyloxy) ethyl)dodecane- 1,12-diaminium bromide (G-12)

Fig. 1 The synthetic route of synthesized gemini surfactants

holder using epoxy resin so that the flat surface was only surface in electrode. Before each measurement, the electrode was immersed in a test solution at open circuit potential (OCP) until a steady state was reached. All polarization curves were recorded by a Voltalab 40 Potentiostat PGZ 301. Each experiment was repeated at

least three times to check the reproducibility. Potentiodynamic polarization measurements were obtained by changing the electrode potential automatically from -1000 to -200 mV versus SCE at open circuit potential with a scan rate 2 mV s^{-1} at 25 °C [24].

Electrochemical impedance spectroscopy (EIS)

EIS measurements were carried out by means of impedance equipment (Voltalab 40 Potentiostat PGZ 301) and controlled with corrosion analysis software. Impedance spectra were obtained in the frequency range 100 kHz–30 mHz with ten points per decade. A sine wave with 10 mV amplitude was used to perturb the system. An SCE was used as reference and a Pt plate was used as a counter electrode. All potentials are reported versus SCE. All experiments were carried out at 25 ± 1 °C. Each experiment was repeated at least three times to check the reproducibility [25].

Weight loss measurements

An analytical balance (Model: HR 200, readability: 0.1 mg and standard deviation: ± 0.2 mg) was used for the gravimetric analysis. The CS sheets of $7 \times 3 \times 0.5$ cm were abraded with a series of emery paper (grade 320–400–600–800–1000–1200) and then cleaned successively with distilled water, ethanol and acetone, and finally dried in dry air. After accurately weighting, the samples were immersed in 250 ml of 1 M HCl solution with and without the addition of different concentrations of cationic surfactant inhibitors at various temperatures: 25, 45, and 60 °C. The temperature for weight loss measurements was controlled by a water bath provided with thermostat control ± 0.5 °C. The steel specimens were taken out after 24 h and then rinsed with distilled water twice and degreased with acetone. Then specimens were immersed in 1.0 M HCl solution for 10 s (chemical method for cleaning rust products), rinsed twice with distilled water, ethanol, and acetone, and finally dried in dry air and accurately weighed. The experiments were carried out in triplicates in order to give a good reproducibility, and the average weight loss of three CS sheets was obtained. All tests in this paper were done under aerated conditions [26].

Biodegradability

Biodegradability test in river water of the gemini cationic surfactant was determined by the surface tension method using a Dü-Nouy tensiometer (Krüss type K6) [23]. In this method, each surfactant was dissolved in river water by a concentration of 100 ppm and incubated at 38 °C. A sample was withdrawn daily (for 28 days), filtered, and the surface tension value was measured. The biodegradation percent (D %) was calculated as follows:

$$D\% = (\gamma_t - \gamma_0)/(\gamma_{bt} - \gamma_0) \times 100 \tag{1}$$

where: γ_t is the surface tension at time t, γ_o is the surface tension at time $= 0$ (initial surface tension), and γ_{bt} is the surface tension of river water without addition of surfactants at time t.

Results and discussion

Characterization of the synthesized inhibitors (G-2, G-6, and G-12)

FTIR spectroscopy

The chemical structure for the synthesized inhibitors was characterized by FTIR spectroscopy in the range 4000–500 cm^{-1} and showed the following absorption bands: 3440 cm^{-1} (OH), 2920 cm^{-1} (CH$_3$), 2845 cm^{-1} (CH$_2$), 2612 cm^{-1} (–N$^+$),1733 cm^{-1} (C=O), 1455 cm^{-1} (CH$_2$)$_n$, 1199 cm^{-1} (C–O).

^{1}H-NMR spectroscopy

^{1}H-NMR spectra of the synthesized gemini cationic surfactants showed signals at 0.88 ppm (t, 6H, 2CH$_3$ as a symmetric molecular terminal group), 1.25 ppm (m, 4H, 2CH$_2$CH$_3$ symmetric molecular terminal group), 1.64 ppm (m, nH, CH$_2$), 1.90 ppm (t, 4H, 2CH$_2$COO symmetric group), 1.99 ppm (t, 2H, CH$_2$CH$_2$COO), 2.08 ppm (t, 4H, N2CH$_2$CH$_2$COO symmetric group), 2.66 ppm (t, 2H, NCH$_2$CH$_2$COO), 2.49 ppm (s, 6H, 2CH$_3$N symmetric group), 2.83 ppm (t, 4H, 2CH$_2$CH$_2$OH symmetric group), 3.50 ppm (t, 4H, CH$_2$2CH$_2$OH symmetric group), 3.19 ppm (t, 4H, N–2CH$_2$CH$_2$ symmetric group), 4.91 ppm (t, 2H, CH2CH2 2OH symmetric group). The only difference between the signals of these compounds was the signal intensity of methylene proton (m, nH, COOCH$_2$ (CH$_2$)$_n$CH$_2$CH$_3$), where the intensity of this signal was increased by increasing the methylene groups (chain length) of the prepared compounds.

Potentiodynamic polarization measurements

Figures 2, 3, 4 show Tafel plots for the steel electrode at its moment of immersion in 1.0 M HCl in the presence and absence of various concentrations of gemini surfactant inhibitors at 25 °C.
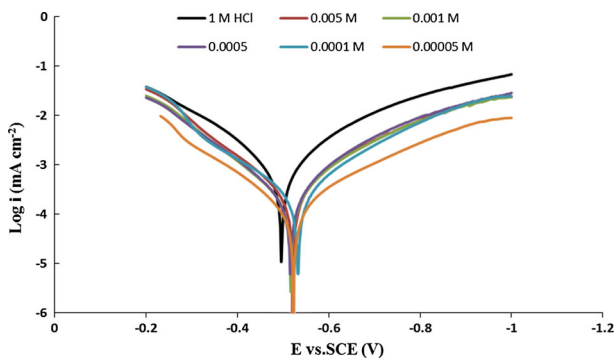

Fig. 2 Polarization curves for carbon steel in 1 M HCl in the absence and presence of different concentrations of inhibitor (G-2) at 25 °C
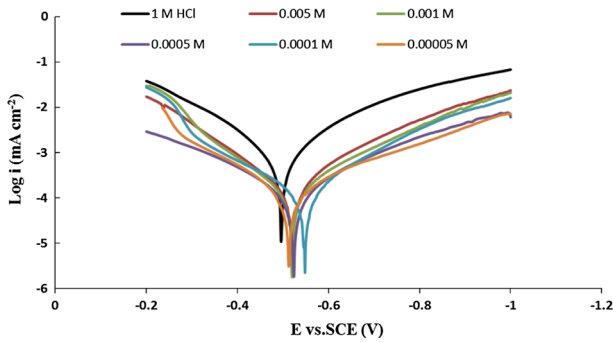
Fig. 3 Polarization curves for carbon steel in 1 M HCl in the absence and presence of different concentrations of inhibitor (G-6) at 25 °C
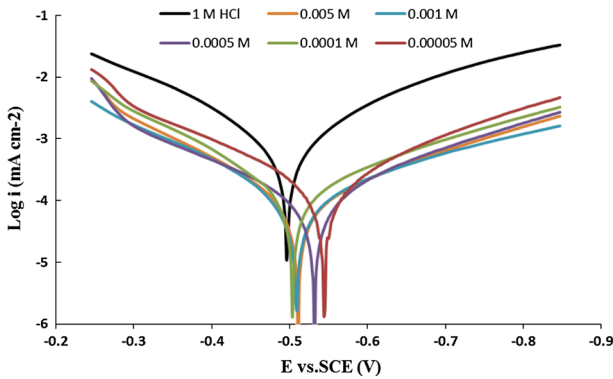

Fig. 4 Polarization curves for carbon steel in 1 M HCl in the absence and presence of different concentrations of inhibitor (G-12) at 25 °C

It was observed that both the cathodic and anodic curves showed lower current density in the presence of inhibitors than those recorded in solutions without inhibitors. This behavior indicated that all used gemini surfactant inhibitors had significant effects on both cathodic and anodic reactions of the corrosion process.

The corrosion parameters including corrosion current densities (i_{corr}, μAcm^{-2}), corrosion potential [E_{corr}, mV(SCE)], cathodic Tafel slope (β_c, $mVdec^{-1}$), and anodic Tafel slope (β_a, $mVdec^{-1}$) derived from this Tafel curves are illustrated in Table 1. It is clear that the presence of the inhibitors causes a marked decrease in the corrosion current density as $i_{corr} = 1325$ μAcm^{-2} for the uninhibited solution where $i_{corr} = 191$, 148, and 84 μAcm^{-2} for G-2, G-6, and G-12 at 5×10^{-3} and 25 °C, respectively. The increase in inhibition efficiency is associated with a shift of both cathodic and anodic branches of the polarization curves towards lower current densities, together with a slight negative shift in E_{corr}, suggest that the three inhibitors act as mixed type inhibitors with predominantly cathodic; i.e. meaning inhibitors reduce the anodic dissolution of mild steel and retard the cathodic

Table 1 Potentiodynamic polarization parameters for corrosion of carbon steel in 1 M HCl in absence and presence of different concentrations of the synthesized gemini surfactants inhibitors at 25 °C

Inhibitor	Conc. of inhibitor (M)	$-E_{corr.}$ (mV(SCE))	$i_{corr.}$ (μAcm^{-2})	β_a (mVdec^{-1})	$-\beta_c$ (mVdec^{-1})	η_p (%)
Absence	0.00	499	1325	202	215	–
G-2	5×10^{-5}	523	475	196	217	64.2
	1×10^{-4}	519	412	194	210	68.9
	5×10^{-4}	518	381	189	184	71.2
	1×10^{-3}	535	385	231	206	70.9
	5×10^{-3}	525	191	201	236	85.6
G-6	5×10^{-5}	523	258	188	207	80.5
	1×10^{-4}	522	191	178	215	85.6
	5×10^{-4}	526	164	246	237	87.6
	1×10^{-3}	550	156	228	187	88.2
	5×10^{-3}	515	148	200	202	88.8
G-12	5×10^{-5}	546	228	219	220	82.8
	1×10^{-4}	506	142	150	232	89.3
	5×10^{-4}	534	136	232	234	89.7
	1×10^{-3}	511	103	164	250	92.2
	5×10^{-3}	513	84	141	209	93.7

hydrogen evolution reaction, but the effect on the cathodic hydrogen evolution reactions surface is more than the anodic dissolution reactions. Inhibition efficiency (η_p, %) was obtained from the following equation [27]:

$$\eta_p\% = \left(\frac{i_{corr} - i_{corr}^0}{i_{corr}}\right) \times 100 \qquad (2)$$

where i_{corr} and i_{corr}^0 are uninhibited and inhibited corrosion current densities, respectively, determined by extrapolation of Tafel lines to the corrosion potential. Data in Table 1 shows that the inhibition efficiency increased with increasing the inhibitor concentrations. The inhibition efficiency of the investigated inhibitors increased in the following order: G-12 > G-6 > G-2. The standard deviation average of three replicate experiments is 0.35.

Electrochemical impedance spectroscopy (EIS)

Figures 5, 6, 7 show the Nyquist diagrams for CS in 1.0 M HCl at 25 °C containing various concentrations of synthesized inhibitors. The charge transfer resistance values (R_{ct}) were calculated from the difference in impedance at lower and higher frequencies [28]. To obtain the double layer capacitance (C_{dl}), values were calculated from the following equation [29]:

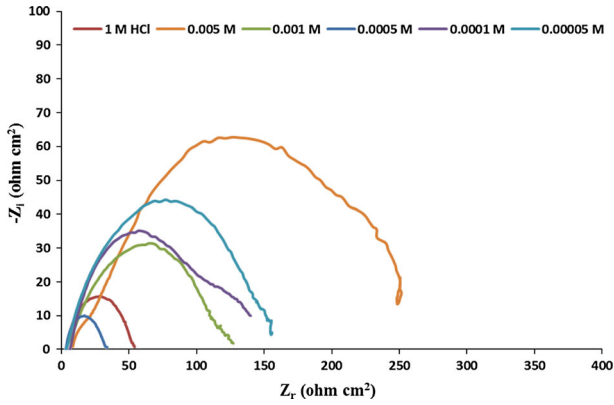$$f_{max} = \frac{1}{2\pi C_{dl} R_{ct}} \qquad (3)$$

Fig. 5 Nyquist plots for CS in 1 M HCl in absence and presence of different concentrations of inhibitor (G-2) at 25 °C
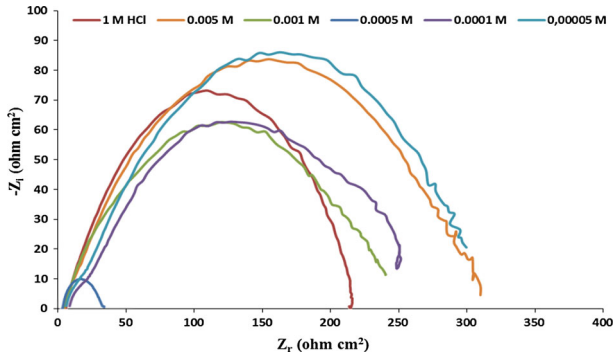

Fig. 6 Nyquist plots for CS in 1 M HCl in absence and presence of different concentrations of inhibitor (G-6) at 25 °C
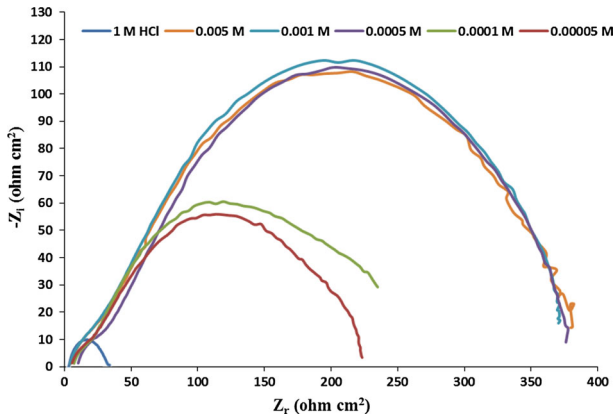

Fig. 7 Nyquist plots for CS in 1 M HCl in absence and presence of different concentrations of inhibitor (G-12) at 25 °C

Table 2 EIS parameters for corrosion of carbon steel in 1 M HCl in absence and presence of different concentrations of the synthesized gemini surfactants at 25 °C

Inhibitor	Conc. of inhibitor (M)	R_s (Ω cm^2)	C_{dl} (μF cm^{-2})	R_{ct} (Ω cm^2)	η_I (%)
Absence	0.00	3.0	119.7	29.8	–
G-2	5×10^{-5}	3.5	100.8	49.9	40.3
	1×10^{-4}	4.0	67.0	118.8	74.9
	5×10^{-4}	5.0	119.0	133.6	77.7
	1×10^{-3}	3.4	104.0	152.7	80.5
	5×10^{-3}	10.5	87.0	255.9	88.4
G-6	5×10^{-5}	6.5	53.8	210.3	85.8
	1×10^{-4}	3.4	92.3	214.4	86.1
	5×10^{-4}	10.5	87.0	255.9	88.4
	1×10^{-3}	9.4	59.1	301.3	90.1
	5×10^{-3}	4.3	58.4	305.0	90.2
G-12	5×10^{-5}	8.7	90.9	220.4	86.5
	1×10^{-4}	7.8	84.1	264.7	88.7
	5×10^{-4}	18.2	199.9	371.4	92.0
	1×10^{-3}	10.9	84.3	377.5	92.1
	5×10^{-3}	10.11	116.0	384.0	92.2

where f_{max} is the frequency at maximum imaginary component of the impedance. In the case of the electrochemical impedance spectroscopy, the inhibition efficiency was calculated using charge transfer resistance according to the following equation [29]:

$$\eta_I = \left(\frac{R_{ct} - R_{ct}^0}{R_{ct}^0} \right) \times 100 \tag{4}$$

where R_{ct} and R_{ct}^0 are the charge transfer resistance values without and with an inhibitor for CS in 1.0 M HCl, respectively.

Various impedance parameters such as charge transfer resistance (R_{ct}, Ω cm^2), double layer capacitances (C_{dl}, μF cm^{-2}) and inhibition efficiency (η_Z) for G-2, G-6, and G-12 were calculated and listed in Table 2.

It was clear that R_{ct} values in the presence of the inhibitor were always greater than their values in the absence of the inhibitor as R_{ct} for uninhabited solution equal to 29.8 Ω cm^2 where $R_{ct} = 49.9, 118.8, 133.6, 152.7,$ and 255.9 Ω cm^2 for G-2 at $5 \times 10^{-5}, 1 \times 10^{-4}, 5 \times 10^{-4}, 1 \times 10^{-3}$, and 5×10^{-3} at 25 °C. Charge transfer resistance, R_{ct}, values increased in the presence of the inhibitor, which indicates a reduction in the steel corrosion rate. The capacitance, C_{dl}, values were decreased due to a decrease in local dielectric constant and/or an increase in the thickness of the electrical double layer, suggesting that the inhibitor molecules acted by adsorption at the metal/solution interface. Addition of synthesized inhibitors provided lower C_{dl} values, probably as a consequence of replacement of water molecules by inhibitor molecule at the electrode surface. Also, the inhibitor
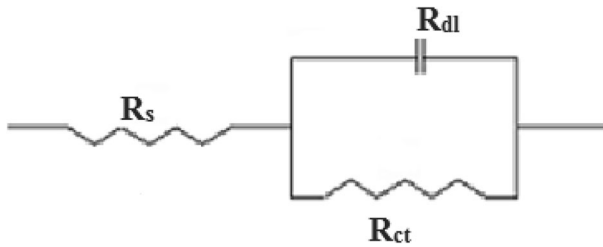
Fig. 8 Electrical equivalent circuit used for modeling the interface Fe/1 M HCl solution without and with the synthesized surfactant inhibitors

molecules may reduce the capacitance by increasing the double layer thickness according to the Helmholtz model [30]:

$$\delta_{org} = \frac{\varepsilon\varepsilon_0 A}{C_{dl}} \tag{5}$$

where ε is the dielectric constant of the medium, ε_0 is the vacuum permittivity, A is the electrode surface area, and δ_{org} is the thickness of the protective layer. C_{dl} value was always smaller in the presence of the inhibitor than in its absence as follows 119.7, 100.8, 67.0, 119.0, 104.0, and 87.0 at 0.0, 5×10^{-5}, 1×10^{-4}, 5×10^{-4}, 1×10^{-3}, and 5×10^{-3} for G-2 at 25 °C, respectively, which may be the result of the effective adsorption of the synthesized inhibitors. The standard deviation average of three replicates was 0.34. The inhibiting efficiency was in the following order: G-12 > G-6 > G-2.

Results obtained from EIS can be interpreted in terms of the equivalent circuit of the electrical double layer shown in Fig. 8, which was used previously to model the iron/acid interface, and a similar circuit have been described in the literature for the acidic corrosion inhibition of steel [31–33].

Weight loss measurements

Effect of inhibitor concentration

The corrosion rate (k) was calculated from the following equation [34]:

$$k = \frac{\Delta W}{St} \tag{6}$$

where ΔW is the average weight loss of three parallel CS sheets, S is the total area of one specimen, and t is immersion time.

The inhibition efficiency (η_w) of the prepared gemini surfactant inhibitors on the corrosion of CS are calculated from the following equation [35]:

$$\eta_w = \left(\frac{W_{corr} - W_{corr}^0}{W_{corr}} \right) \times 100 \tag{7}$$

where W and W$_o$ are the weight loss of CS in the absence and presence of the inhibitors, respectively.
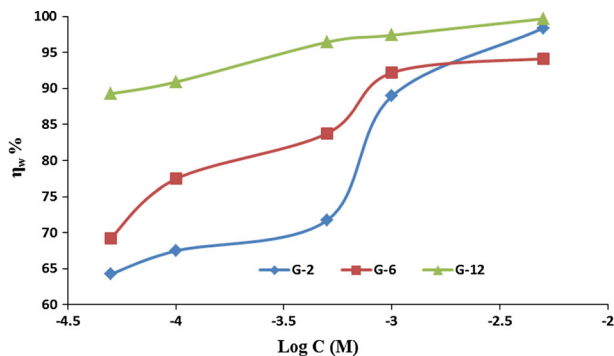
Fig. 9 Variation of the inhibition efficiency with different concentrations of the synthesized inhibitors in 1 M HCl at 25 °C

Figure 9 shows the inhibition efficiency values of CS with different concentrations of the synthesized inhibitors in 1.0 M HCl solution at 25 °C. The corrosion inhibition enhances with the inhibitor concentration. This behavior is because the adsorption coverage of inhibitor on CS surface increases with the inhibitor concentration.

Effect of temperature

The effect of temperature on the corrosion parameters of CS in free and inhibited solutions of 1.0 M HCl was studied at a temperature range of 25–60 °C. Acid solutions were inhibited by adding different concentrations of inhibitors (G-2, G-6, or G-12). The obtained corrosion parameters are given in Table 3 and shows that when temperature increases, in the absence and presence of inhibitor, the corrosion rate increases. Also, the data in Table 3 show that the corrosion rate of steel increased with increasing temperature for both uninhibited and inhibited solution. The corrosion rate of steel increased rapidly with increasing temperature in the absence of the inhibitors. Figure 10 reveals that the inhibition efficiency decreases with increases of temperature.

The results obtained from the weight loss measurements were in good agreement with those obtained from the potentiodynamic polarization and EIS methods.

Adsorption isotherm

Basic information on the interaction between inhibitor and steel surface can be provided by the adsorption isotherm. Attempts were made to fit to various isotherms including Frumkin, Langmuir, Temkin, Freundlich, Bockris-Swinkels, and Flory–Huggins isotherms. By far, the results are best fitted by the Langmuir adsorption isotherm equation [36, 37]:

$$\frac{C}{\theta} = \left(\frac{1}{K_{ads}}\right) + C \tag{8}$$

Table 3 Weight loss data for carbon steel in 1 M HCl without and with different concentrations of synthesized surfactants at various temperatures

| Inhibitor	Conc. inhibitor (M)	25 °C			45 °C			60 °C		
		k (mg cm^{-2} h^{-1})	θ	η_w (%)	k (mg cm^{-2} h^{-1})	θ	η_w (%)	k (mg cm^{-2} h^{-1})	θ	η_w (%)
Absence	0.00	0.034	–	–	0.530	–	–	1.520	–	–
G-2	5×10^{-5}	0.012	0.64	64.2	0.202	0.62	61.8	0.432	0.72	71.57
	1×10^{-4}	0.011	0.67	67.5	0.080	0.85	84.9	0.240	0.84	84.22
	5×10^{-4}	0.010	0.72	71.7	0.064	0.88	87.9	0.165	0.89	89.13
	1×10^{-3}	0.004	0.89	88.9	0.054	0.90	89.8	0.149	0.90	90.22
	5×10^{-3}	0.001	0.98	98.4	0.043	0.92	91.8	0.109	0.93	92.80
G-6	5×10^{-5}	0.010	0.69	69.4	0.115	78.3	36.5	0.343	0.77	77.42
	1×10^{-4}	0.008	0.77	77.2	0.061	88.5	39.1	0.232	0.85	84.77
	5×10^{-4}	0.006	0.84	83.7	0.055	89.5	71.7	0.090	0.94	94.11
	1×10^{-3}	0.003	0.92	92.2	0.042	92.1	77.9	0.084	0.94	94.46
	5×10^{-3}	0.002	0.94	94.1	0.041	92.2	84.0	0.069	0.95	95.48
G-12	5×10^{-5}	0.004	0.89	89.3	0.090	0.83	83.0	0.303	0.80	80.05
	1×10^{-4}	0.003	0.91	90.9	0.071	0.87	86.5	0.223	0.85	85.33
	5×10^{-4}	0.001	0.96	96.4	0.065	0.88	87.7	0.178	0.88	88.32
	1×10^{-3}	0.001	0.97	97.4	0.046	0.91	91.4	0.152	0.90	90.01
	5×10^{-3}	0.0001	0.99	99.7	0.038	0.93	92.9	0.062	0.96	95.90
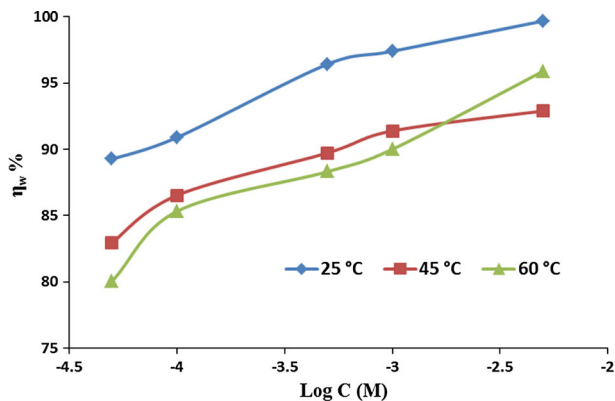
Fig. 10 Effect of the temperature on the inhibition efficiency was obtained by weight loss method for carbon steel in 1 M HCl in the presence of different concentrations of inhibitor (G-12)
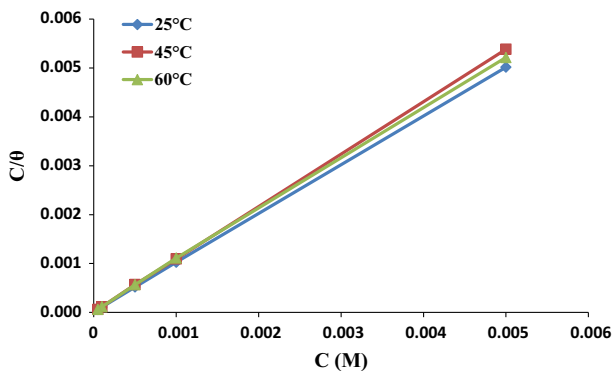

Fig. 11 Langmuir isotherm adsorption model of inhibitor (G-12) on the carbon steel surface in 1 M HCl at different temperatures

where C is the inhibitor concentration, K_{ads} is the adsorptive equilibrium constant and θ is the surface coverage calculated from weight loss data as: $\theta = ([W - W_0]/W_0)$ where W and W_0 are the weight loss of CS in the absence and presence of the inhibitors, respectively.

The surface coverage (θ) for G-12 was tested graphically for fitting into a suitable adsorption isotherm as indicated in Fig. 11. Plotting C/θ versus C yielded a straight line with a correlation coefficient (R^2) of 0.999, 1, and 1, for G-2 at 25, 45, and 60 °C, respectively and a slope closed to one as seen in Table 4. Similar plots are obtained for G-2 and G-6 this indicates that the adsorption of these inhibitors can be fitted to a Langmuir adsorption isotherm. The strong correlation of the Langmuir adsorption isotherm may confirms the validity of this approach.

The equilibrium constant (K_{ads}) for the adsorption–desorption process of these compounds can be calculated from reciprocal of the intercept. The adsorptive equilibrium constant (K_{ads}) values are listed in Table 4. It is clear that the large

Table 4 Thermodynamic parameters of adsorption on carbon steel surface in 1 M HCl containing different concentrations of the synthesized gemini inhibitors

Inhibitor	Temperature (°C)	Slope	R^2	K_{ads} $(M^{-1}) \times 10^3$	ΔG^0_{ads} $(kJ\ mol^{-1})$	ΔH^0_{ads} $(kJ\ mol^{-1})$	ΔS^0_{ads} $(J\ mol^{-1}K^{-1})$
G-2	25	1.00	0.999	10	−32.77	37.47	110.09
	45	1.08	1	50	−39.22		123.35
	60	1.07	1	50	−41.07		123.35
G-6	25	1.06	0.999	25	−35.04	31.65	117.69
	45	1.08	1	111	−41.34		129.99
	60	1.04	1	100	−42.99		129.11
G-12	25	1.00	1	100	−38.47	30.70	129.21
	45	1.07	1	50	−39.22		123.35
	60	1.04	0.999	33	−39.95		119.98

values indicate a strong adsorption of the synthesized inhibitors on the surface of CS in 1.0 M HCl.

Standard thermodynamic adsorption parameters

Thermodynamic parameters play important role in understanding the inhibitive mechanism. Thus, the standard adsorption free energy (ΔG^0_{ads}) can be obtained according to the following equation [38–42]:

$$\Delta G^0_{ads} = -RT \ln(55.5 K_{ads}) \tag{9}$$

where R is the gas constant (8.314 J mol^{-1} K^{-1}), T is the absolute temperature, and the value 55.5 is the concentration of water in solution expressed in M.

The negative values of ΔG^0_{ads} indicate that the adsorption of inhibitor molecule onto a steel surface is a spontaneous process. Generally, values of ΔG^0_{ads} up to 20 k J mol^{-1} are consistent with the electrostatic interaction between the charged molecules and the charged metal (physical adsorption) while those more negative than −40 kJ mol^{-1} involve sharing or transfer of electrons from the inhibitor molecules to the metal surface to form a co-ordinate type of bond (chemisorption) [43–45]. In the present study, the calculated ΔG^0_{ads} values in Table 4 ranged between −32.77 and −42.99 kJ mol^{-1}. This indicates that both physical and chemical adsorptions took place [46].

The adsorption heat can be calculated according to the Van't Hoff equation [47]:

$$\ln K_{ads} = \left(\frac{-\Delta H^0_{ads}}{RT} \right) + \text{constant} \tag{10}$$

where ΔH^0_{ads} and K_{ads} are the adsorption heat and adsorptive equilibrium constant, respectively.

To obtain the standard enthalpy, plotting ln K_{ads} versus 1/T (Fig. 12) yielded straight line according to Eq. (10) with slope equal to $-\Delta H^0_{ads}/R$. The ΔH^0_{ads} values were equal to 37.47, 31.65, and 30.70 kJ mol^{-1} for G-2, G-6, and G-12,

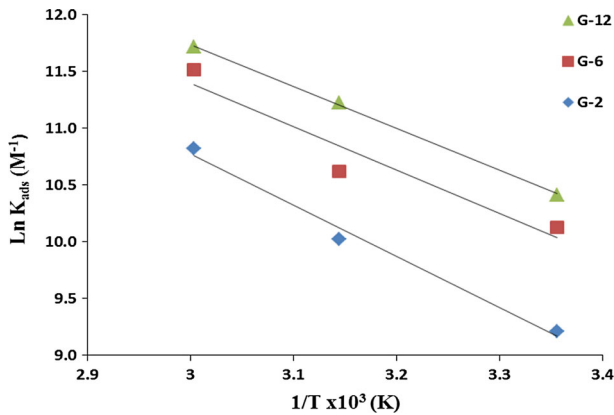**Fig. 12** The relationship between ln K_{ads} and 1/T for carbon steel in 1 M HCl solution containing different concentrations of inhibitors

respectively. The positive values of ΔH^0_{ads} indicated that the adsorption of the inhibitors on the CS surface is endothermic.

Entropy of inhibitor adsorption ΔS^0_{ads} can be calculated using the following equation [48]:

$$\Delta G^0_{ads} = \Delta H^0_{ads} - T\Delta S^0_{ads} \tag{11}$$

The obtained ΔS^0_{ads} values were listed in Table 4. The positive values of ΔS^0_{ads} mean that the adsorption process is accompanied by an increase in entropy, as was expected, since the endothermic adsorption process is always accompanied by an increase in entropy, which is the driving force for the adsorption of inhibitor onto the CS surface e.g. ΔS^0_{ads} = 110.09, 123.35, and 123.35 J mol^{-1} K^{-1} at 25, 45, and 60 °C, respectively for G-2 [49].

Activation parameters

The activation energy of corrosion process with and without the inhibitor was calculated according to the following equation [50]:

$$k = A\exp\left(\frac{-E_a}{RT}\right) \tag{12}$$

where E_a represents the apparent activation energy, R is the gas constant, T is the absolute temperature, A is the pre-exponential factor, and k is the corrosion rate.

The regression between ln k and 1/T was calculated, and Arrhenius plots of ln k versus 1/T for the blank and different concentrations of the synthesized inhibitor G-12 (representative sample) were shown in Fig. 13.

Figure 13 and showed that all the linear regression coefficients (R^2) are very close to 1, which means the linear relationship between ln k and 1/T is good. The value of E_a in the presence of all synthesized inhibitors is higher than that in the
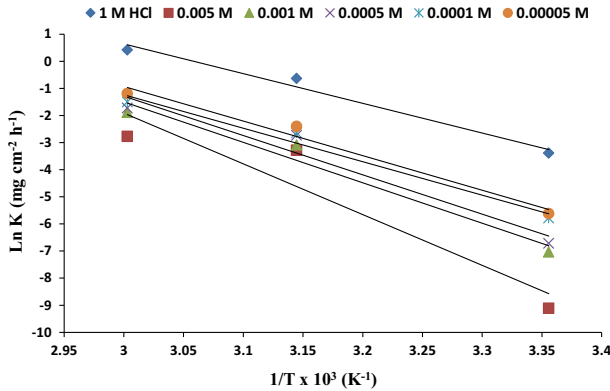
Fig. 13 ln k versus $1/T$ curves for carbon steel dissolution in absence and presence of different concentrations of inhibitor (G-12) in 1 M HCl solution

uninhibited acid solution; e.g. E_a = 91.10, 59.22, 67.69, 73.04, 88.19, and 128.38 kJ mol^{-1} at 0.0, 5×10^{-5}, 1×10^{-4}, 5×10^{-4}, 1×10^{-3} , and 5×10^{-3} mM for G-2, respectively, as in Table 5. Many studies [51, 52] showed E_a increased in the presence of inhibitor than in the absence of inhibitor in contrast to other studies [53–55].

Equation (12) showed that, $-E_a/R$ is the slope of the straight line (ln k vs. $1/T$), so the value of E_a could elucidate the effect of temperature on corrosion inhibition. E_a increased with increase in the inhibitors concentration, which further confirms that efficiency decreases with increase in temperature. This behavior indicates that the adsorption of the inhibitors on the CS in 1.0 M HCl is physical adsorption.

Enthalpy and entropy of activation (ΔH^* and ΔS^*) were calculated from the transition state theory [56] and listed in Table 5.

$$\ln\left(\frac{k}{T}\right) = \left(\ln\left(\frac{R}{N_A h}\right) + \left(\frac{\Delta S^*}{R}\right)\right) - \frac{\Delta H^*}{RT} \tag{13}$$

where h is Planck's constant, N_A is Avogadro's number, R is the universal gas constant, ΔH^* is the enthalpy of the activation, and ΔS^* is the entropy of activation. Plotting of ln (k/T) against $1/T$ (Eq. 13) for CS dissolution in 1.0 M HCl in the absence and presence of different concentrations from the synthesized inhibitors, gave straight lines, as illustrated in Fig. 14. Data in Table 5 represented the values of ΔH^* and ΔS^*, which were calculated from the slope of $-\Delta H^*/R$ and the intercept of [ln($R/N_A h$) + $\Delta S^*/R$] of the straight lines. Values of ΔH^* and ΔS^* were calculated and listed in Table 5. Inspection of these data revealed that the positive signs of the enthalpy (ΔH^*) reflected the endothermic nature of the steel dissolution process and indicated that the dissolution of steel was difficult [57]. It is clear that from Table 5 that ΔS^* values in the presence of the synthesized cationic inhibitors have positive sign, which means that an increase in ordering takes place in going from reactants to the M_{ads} reaction complex.

Table 5 Activation parameters values for carbon steel in 1 M HCl in the absence and presence of different concentrations of the synthesized gemini inhibitors

Inhibitor	Conc. of inhibitor (M)	E_a (kJ mol^{-1})	ΔH^*_{ads} (kJ mol^{-1})	ΔS^*_{ads} (J mol^{-1} K^{-1})
Absence	0.00	91.10	88.49	24.95
G-2	5×10^{-5}	59.22	100.06	44.09
	1×10^{-4}	67.69	103.38	56.59
	5×10^{-4}	73.04	117.98	97.37
	1×10^{-3}	88.19	121.40	105.91
	5×10^{-3}	128.38	153.04	197.37
G-6	5×10^{-5}	54.98	61.68	4.52
	1×10^{-4}	67.16	70.14	27.36
	5×10^{-4}	67.66	77.34	31.20
	1×10^{-3}	83.68	78.98	46.48
	5×10^{-3}	86.35	85.52	78.10
G-12	5×10^{-5}	100.18	96.67	34.94
	1×10^{-4}	102.68	100.03	47.61
	5×10^{-4}	120.59	112.59	82.18
	1×10^{-3}	124.01	116.57	92.55
	5×10^{-3}	155.65	142.75	167.18
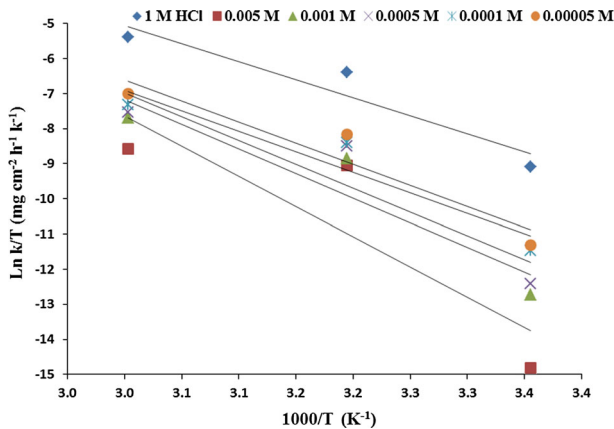
Fig. 14 Arrhenius plots of ln (k/T) versus $1/T$ for carbon steel in 1 M HCl solution without and with different concentrations of the synthesized inhibitor (G-12)

Biodegradation

Some gemini cationic surfactants have potential promise as new candidates for environmentally friendly surfactants. Dialkylammonium salts have been widely used in industrial and household products. Increasing usage, however, is causing environmental problems owing to poor biodegradability. Thus, much attention has

been paid to the development of novel surfactants. A new type of hydrolyzable cationic gemini surfactants, containing oxycarbonyl groups in the lipophile, may be much more easily hydrolyzed [58].

However, modification of the structure or addition of a natural origin substituent can significantly affect biodegrability. Compounds containing easily hydrolyzed groups in the structure showed a good biodegradability. Introduction of the carbonate linkage into the hydrophobic moiety of gemini surfactants enhanced its biodegradability.

The biodegradability of the synthesized gemini surfactants was evaluated using surface tension method. All the prepared surfactants under investigation have the same hydrophobic part, hence the hydrophilic head group and oxycarbonyl group are the main factors affecting this process. Comparing the results of the biodegradation Die-Away test in river water (Table 6) and the surface tension values reflect the fact that lowering of the surface tension is a reverse function of biodegradation.

It is clear from data in Table 6 that the biodegradation ratio of all of the synthesized compounds ranged from 71 to 80 % after the 28th day of expose to the microorganisms. Furthermore, the highest biodegradation extent was obtained for G-2 and G-6 at 80 and 75 % compared to G-12 surfactants at 71 %. As concluded from the biodegradation ratios, the values meet the international recommendation of the biodegradable surfactants in drain water which is 70 % after 28 days [59].

A comparison of the biodegradability of surfactants with two, six, and 12 methylene groups in the spacer showed a much higher degree of biodegradation for the former compounds, in addition to containing a carbonate group in the tail. This is due to the electron density of the carbonyl carbon.

Very low biodegradation percentages found for gemini surfactants with dodecane spacer length can be explained by assuming that dicationic substances with a high number of carbons (12) between the nitrogen and hydrophobic tail (giving a large hydrophobic moiety) are non-biodegradable. The highest biodegradation percentages were found with gemini surfactants obtained from G-2 because of small hydrophobic character.

It is clear that there is a direct relationship between the number of methylene groups in the spacer and the percent of biodegradation. Consequently, these surfactants can be classified as biodegradable surfactants. In fact, the biodegradation affinity is due to the presence of an oxycarbonyl group which has the ability to degrade by the action of the environmental microorganisms.

Table 6 The biodegradation ratio of all the synthesized gemini cationic surfactants in river water at 25 °C

Compound	Biodegradation (%) after 28 day
G-2	80
G-6	75
G-12	71

The simplest pathway of the degradation considered in case of the studied compounds is the bacterial attack at the far end of either the hydrophobic chain, or a central fission separating the hydrophobic and the spacer chain [60].

Mechanism of inhibition

The adsorption of organic molecules on solid surfaces cannot be considered only a purely physical or a purely chemical adsorption phenomenon. In physical adsorption, the inhibitor molecules can be adsorbed on the steel surface via electrostatic interaction between the charged metal surface and charged inhibitor molecule. While chemical adsorption arises from the donor–acceptor interactions between free electron pairs of the heteroatoms and π-electrons of multiple bonds, as well as phenyl group and vacant d-orbitals of iron, it has been reported that the adsorption of compounds and the orientation of molecules could be dependent on the pH and/or electrode potential [61]. The free energy value of adsorption was around -40 kJ mol^{-1} , indicating the physicochemical adsorption of the synthesized inhibitors. The large size and high molecular weight of synthesized molecules can also contribute to the greater inhibition efficiency of the studied surfactant inhibitors. According to the large size of the alkyl chain, the inhibition efficiency order was G-12 > G-6 > G-2, and can be interpreted by the formation of a more efficient protective layer at the surface of CS surface, which increases the surface coverage values resulting in displacement of water molecules as well as ions adsorbed on the surface.

The corrosion process occurred between the metal surface and the aggressive molecules at the negatively charged centers at the metal surface. The cationic inhibitor molecules are believed to be adsorbed at the metal surface when present in the medium. The adsorption occurs between the positively charged centers at the surface and also at the edges of the metal fabricates. That adsorption forms what is called the sweaty layer of the inhibitor molecules at the metal surface. The extent of the arrangement and the degree of the coverage of inhibitor molecules at the metal surface determine the efficiency of the inhibitor.

The influence of the chain length on the corrosion process can be explained as the result of the repulsion between the nonpolar hydrophobic species and the polar medium. Because of this repulsion, the hydrophobic chains are directed to the metal/water interface and form a well ordered layer. Hence, the repulsion force between the chains and the aggressive medium will increase by increasing the number of methylene groups [62].

The increase in inhibition efficiency is associated with a shift of both cathodic and anodic branches of the polarization curves towards lower current densities, together with a slight positive shift in E_{corr}, less than 85 mV with increasing concentration, suggest that the three inhibitors act as mixed type inhibitors that are predominantly anodic; i.e. meaning inhibitors reduce the anodic dissolution of mild steel and retard the cathodic hydrogen evolution reaction, but the effect on the anodic dissolution reactions is more than on the cathodic hydrogen evolution reactions.

The anodic Tafel slope (β_a) and cathodic Tafel slope (β_c) of the used cationic surfactants were slightly changed with inhibitor concentrations; this indicates that these inhibitors affected both the anodic and cathodic reactions; the slight change upon increasing inhibitor concentrations indicate that the presence of prepared cationic surfactants don't change the reaction mechanism of inhibition.

It was found that the current density I_{corr} values decrease considerably in the presence of an inhibitor, and as the inhibitor concentration increases, the corrosion current density is decreasing, and correspondingly η increases.

Surface activity–corrosion inhibition efficiency relationship

The relation between the surface activity and corrosion inhibition was established in previous works [63–65]. Presence of the hydrophobic chain length of the inhibitor molecules increases their surface activity and the tendency towards adsorption at the interfaces. Moreover, increasing the adsorption tendency increases the amounts of adsorbed molecules onto the metal surface, which consequently increases the surface coverage values. As a result, the metal surface is protected from dissolution. The critical micelle concentration (CMC) is a key indicator in determining the effectiveness of surfactants as corrosion inhibitors. Below the CMC, individual surfactant molecules or monomers tend to adsorb on exposed interfaces, so interfacial aggregation reduces surface tension and is related to corrosion inhibition. Above the CMC, the surface becomes covered with more than one monolayer and forms a protection layer on the metal surface. Thus, any additional surfactant added to the solution above the CMC will lead to the formation of micelles or multiple adsorbed layers on surfaces. Consequently, the surface tension and corrosion current density are not altered significantly above the CMC. Therefore, an excellent surfactant inhibitor is one that aggregates or adsorbs at low concentrations. In other words, surfactants with low CMC values are desirable because they adsorb at low concentrations [66].

Also, increasing the surface activity of the inhibitor solutions is accompanied by a decrease in the CMC values and increases the hydrophobic character, as well as increases inhibition efficiency, such as when the CMC values are 0.380, 0.389, and 0.431 mM at 25 °C for G-12, G-6, and G-2, respectively, the inhibition efficiency is 64.2, 69.4, and 89.3 % at 5×10^{-5} and at 25 °C for G-2, G-6, and G-12, respectively.

Conclusions

(1) Gemini cationic surfactants exhibited effective inhibiting properties for CS corrosion in 1.0 M HCl solution. The inhibition efficiency increased with increasing the concentration of inhibitors.

(2) Potentiodynamic polarisation results revealed that G-2, G-6, and G-12 in 1.0 M HCl solution acted as a mixed-type inhibitor, which decreases the cathodic, anodic, and corrosion currents to a great extent.

(3) EIS measurement results indicate that the resistance of the CS electrode increases greatly, and its capacitance decreases by increasing the inhibitor concentration.

(4) Data obtained from weight loss and EIS measurements are in good agreement with those of the polarisation resistance method.

(5) The effect of temperature on corrosion inhibition efficiency of the synthesized inhibitors has been investigated, showing that the inhibition efficiency decreases with increasing temperature.

(6) The adsorption of G-2, G-6, or G-12 on the CS surface from hydrochloric acid solutions obeys the Langmuir adsorption isotherm model.

(7) Increasing the surface activity of the inhibitor solutions is accompanied by an increase in the inhibition efficiency.

References

1. L. Afia, R. Salghi, E.I.H. Bazzi, A. Zarrouk, B. Hammouti, M. Bouri, H. Zarrouk, L. Bazzi, L. Bammou, Res. Chem. Intermed. **38**, 1707 (2012)
2. H.B. Ouici, O. Benali, Y. Harek, L. Larabi, B. Hammouti, A. Guendouzi, Res. Chem. Intermed. **39**, 3089 (2013)
3. K.F. Khaled, E. Ebenso, Res. Chem. Intermed. (2013). doi:10.1007/s11164-013-1167-3
4. A. Khadraoui, A. Khelifa, H. Hamitouche, R. Mehdaoui, Res. Chem. Intermed. **40**, 9614 (2014)
5. A. Khadraoui, A. Khelifa, Res. Chem. Intermed. (2012). doi:10.1007/s11164-012-0910-5
6. A. Khadraoui, A. Khelifa, Res. Chem. Intermed. **39**, 3937 (2013)
7. G. Karthik, M. Sundaravadivelu, P. Rajkumar, Res Chem Intermed. doi:10.1007/s11164-013-1291-0
8. M.M. Deshpande, S.B. Junne, D.V. Saraf, P.A. Kulkarni, J. Chem. Pharm. Res. **2**(3), 453 (2010)
9. A. Popova, E. Sokolova, S. Raicheva, M. Christov, Corros. Sci. **45**, 33 (2003)
10. R. Solmaz, G. Kardas, B. Yazıcı, M. Erbil, Colloids Surf. A Physico. Chem. Eng. Asp. **312**, 7 (2008)
11. I. Aiad, S.M. Tawfik, S.M. Shaban, A. Abd-Elaal, M. El-Shafie, J. Surfactants Deterg. **17**, 391 (2014)
12. A. Abd-Elaal, I. Aiad, S.M. Shaban, S.M. Tawfik, A. Sayed, J. Surfactants Deterg. **17**, 483 (2014)
13. S.M. Shaban, A. Sayed, S.M. Tawfik, A. Abd-Elaal, I. Aiad, J. Ind, Eng. Chem. **19**, 2004 (2013)
14. S.M. Tawfik, J. Mol. Liq. **207**, 185 (2015)
15. N.A. Negm, S.M. Tawfik, E.A. Badr, M.I. Abdou, F.M. Ghuiba, J. Surfactants Deterg. **18**, 413 (2015)
16. N.A. Negm, F.M. Ghuiba, S.A. Mahmoud, S.M. Tawfik, Eng. Life Sci. **11**(5), 496 (2011)
17. N.A. Negm, Y.M. Elkholy, M.K. Zahran, S.M. Tawfik, Corros. Sci. **52**, 3523 (2010)
18. N.A. Negm, F.M. Ghuiba, S.M. Tawfik, Corros. Sci. **53**, 3566 (2011)
19. S.M. Tawfik, A. Sayed, I. Aiad, J Surfactants Deterg. **15**, 577 (2012)
20. F. Bentiss, F. Gassama, D. Barbry, L. Gengembre, H. Vezin, M. Lagrenee, M. Traisnel, Appl. Surf. Sci. **252**, 2684 (2006)
21. A. Ouchrif, M. Zegmout, B. Hammouti, A. Dafali, M. Benkaddour, A. Ramdani, S. Elkadiri, Prog. Org. Coat. **53**, 292 (2005)
22. G.H. Sayed, F.M. Ghuiba, M.I. Abdou, E.A. Badr, S.M. Tawfik, N.A. Negm, J. Surfactants Deterg. **15**, 735 (2012)
23. S.M. Tawfik, J. Ind. Eng. Chem. (2015). doi:10.1016/j.jiec.2015.02.011
24. M.A. Hegazy, M.F. Zaky, Corros. Sci. **52**, 1333 (2010)
25. I. Aiad, M.M. El-Sukkary, E.A. Soliman, M.Y. El-Awady, S.M. Shaban, J. Ind. Eng. Chem. **20**, 3524 (2014)
26. N.A. Negm, E.A. Badr, S.M. Tawfik, A.F. El Farargy, J. Appl. Chem. **7**(6), 13 (2014)
27. S.M. Tawfik, M.F. Zaky, Res. Chem. Intermed. (2015). doi:10.1007/s11164-015-1926-4
28. Q. Qu, L. Li, W. Bai, S. Jiang, Z. Ding, Corros. Sci. **512**, 423 (2009)
29. S. Haruyama, T. Tsuru, B. Gijutsu, J. Jpn. Soc. Corros. Eng. **27**, 573 (1978)

30. M.A. Hegazy, Corros. Sci. **51**, 2610 (2009)
31. A.M. Atta, O.E. El-Azabawy, H.S. Ismail, M.A. Hegazy, Corros. Sci. **53**, 1680 (2011)
32. R.A. Prabhu, T.V. Venkatesha, A.V. Shanbhag, G.M. Kulkarni, R.G. Kalkhambkar, Corros. Sci. **50**, 3356 (2008)
33. M. Elayyachy, A. El Idrissi, B. Hammouti, Corros. Sci. **48**, 2470 (2006)
34. H.D. Lece, K.C. Emregul, O. Atakol, Corros. Sci. **50**, 1460 (2008)
35. H.B. Ouici, O. Benali, Y. Harek, L. Larabi, B. Hammouti, A. Guendouzi, Res. Chem. Intermed. **39**, 2780 (2013)
36. A. Gülşen, Res. Chem. Intermed. **38**, 1312 (2012)
37. O.K. Abiola, J.O.E. Otaigbe, Corros. Sci. **51**, 2790 (2009)
38. E.E. Oguzie, C. Unaegbu, C.N. Ogukwe, B.N. Okolue, A.I. Onuchukwu, Mater. Chem. Phys. **84**, 363 (2004)
39. S.K. Shukla, M.A. Quraishi, Corros. Sci. **51**, 1007 (2009)
40. G. Moretti, F. Guidi, G. Grion, Corros. Sci. **46**, 387 (2004)
41. S.M.A. Hosseini, A. Azimi, Corros. Sci. **51**, 728 (2009)
42. P.C. Okafor, Y. Zheng, Corros. Sci. **51**, 850 (2009)
43. E. Cano, J.L. Polo, A. La Iglesia, J.M. Bastidas, Adsorption **10**, 219 (2004)
44. F. Bentiss, M. Lebrini, M. Lagrenee, Corros. Sci. **47**, 2915 (2005)
45. W.H. Li, Q. He, S.T. Zhang, C.L. Pei, B.R. Hou, J. Appl. Electrochem. **38**, 289 (2008)
46. E. Bensajjay, S. Alehyen, M. El Achouri, S. Kertit, Anti-Corros. Methods Mater. **50**, 402 (2003)
47. E.A. Noor, A.H. Al-Moubaraki, Mater. Chem. Phys. **110**, 145 (2008)
48. T.P. Zhao, G.N. Mu, Corros. Sci. **41**, 1937 (1999)
49. A.M. Badawi, M.A. Hegazy, A.A. El-Sawy, H.M. Ahmed, W.M. Kamel, Mater. Chem. Phys. **124**, 458 (2010)
50. H. Ashassi-Sorkhabi, B. Shaabani, D. Seifzadeh, Appl. Surf. Sci. **239**, 154 (2005)
51. M.M. Saleh, Mater. Chem. Phys. **98**, 83 (2006)
52. A. Popova, M. Christov, A. Vasilev, Corros. Sci. **49**, 3276 (2007)
53. H. Ashassi-Sorkhabi, B. Shaabani, D. Seifzadeh, Electrochim. Acta **50**, 3446 (2005)
54. M.S. Morad, A.M. Kamal, El-Dean. Corros. Sci. **48**, 3398 (2006)
55. A.S. Fouda, A.A. Al-Sarawy, E.E. El-Katori, Desalination **2011**, 5 (2006)
56. S. Şafak, B. Duran, A. Yurt, G. Türkoğlu, Corros. Sci. **54**, 251 (2012)
57. A.A. Al-Sarawy, A.S. Fouda, W.A. Shehab, El-Dein. Desalination **229**, 279 (2008)
58. R. Puchta, P. Krings, P. Sandkuhler, Tenside Surfactants Deterg. **30**, 186 (1993)
59. J.S. Leal, J.J. Gonzalez, K.L. Kaiser, V.S. Palabrica, F. Comelles, M.T. Garcia, Acta Hydrochim. Hydrobiol. **22**, 13 (1994)
60. C.G. Van Ginkel, Biodegradation of cationic surfactants. An environmental perspective, in *Handbook of detergents. Part B: Environmental Impact*, vol. 5, ed. by U. Zoller (Marcel Dekker, New York, 2004), p. 533
61. N.A. Negm, S.M. Tawfik, J. Ind. Eng. Chem. **20**, 4463 (2014)
62. N.A. Negm, Y.M. Elkholy, F.M. Ghuiba, M.K. Zahran, S.A. Mahmoud, S.M. Tawfik, J Adsorp Sci Technol. **32**, 512 (2011)
63. S.M. Tawfik, M.F. Zaki, Res. Chem. Intermed. (2014). doi:10.1007/s11164-014-1867-3
64. N.A. Negm, M.A.I. Salem, M.F. Zaki, J. Dis. Sci. Technol. **30**, 1167 (2009)
65. N.A. Negm, A.S. Mohamed, J. Surfactants. Deterg. **7**, 23 (2004)
66. M.A. Malik, M.A. Hashim, F. Nabi, S.A. AL-Thabaiti, Z. Khan, Int. J. Electrochem. Sci. **6**, 1927 (2011)